Acta Crystallographica Section D
Biological Crystallography
ISSN 0907-4449

Structures of R- and T-state hemoglobin Bassett: elucidating the structural basis for the low oxygen affinity of a mutant hemoglobin

Martin K. Safo,[a]* Osheiza Abdulmalik,[b] Hsiang-Ru Lin,[a] Toshio Asakura[b] and Donald J. Abraham[a]

[a]Department of Medicinal Chemistry, School of Pharmacy and Institute for Structural Biology and Drug Discovery, Virginia Commonwealth University, Richmond, VA 23298, USA, and [b]Division of Hematology, Children's Hospital of Philadelphia, PA 19104, USA

Correspondence e-mail: msafo@mail2.vcu.edu

Received 27 October 2004
Accepted 22 November 2004

PDB References: R-state Hb Bassett, 1r1x, r1r1xsf; T-state Hb Bassett, 1r1y, r1r1ysf.

The crystal structures of R- and T-state hemoglobin (Hb) Bassett have been determined to 2.15 and 1.80 Å resolution, respectively. Physiologically, Hb Bassett (αAsp94→Ala) is characterized by a low affinity for oxygen, a reduced Bohr effect and low cooperativity, as well as being slightly unstable (compared with normal adult hemoglobin; HbA). Comparisons between the Hb Bassett structures and previously determined R- and T-state HbA structures revealed that this mutant shares similar tertiary and quaternary structures with other Hbs. However, this analysis did identify localized structural differences between R-state Hb Bassett and R-state HbA at the $\alpha1\beta2$ ($\alpha2\beta1$) dimer interface and at the β-cleft. Specifically, the β-FG corner has shifted closer to the α-C helix in the mutant R structure. In addition, four intersubunit hydrogen bonds found at the $\alpha1\beta2$ interfaces of native R-state Hb structures are abolished or weakened and subsequently replaced by two new intersubunit hydrogen bonds in R-state Hb Bassett. Remarkably, the newly formed hydrogen bonds in the R-state mutant structure are also observed in T-state Hb structures. At the β-cleft, βHis46, which is known to contribute to the Bohr effect in Hb, makes a unique hydrogen-bonding interaction with βAsn139 in the R-state Hb Bassett. Unlike the R-state mutant, the T-state Hb Bassett structure does not display any significant structural changes at both the $\alpha1\beta2$ ($\alpha2\beta1$) dimer interface and the β-cleft. Quite significantly, the mutation has led to removal of an interdimer repulsion involving α1Asp94 and β2Asp99. The R- and T-state structures of Hb Bassett suggest a stereochemical basis for the observed functional properties of this mutant.

1. Introduction

Hemoglobin is an allosteric tetrameric ($\alpha1\beta1$-$\alpha2\beta2$) protein that exists in equilibrium between two alternative structures, the T (tense) state, which possesses low oxygen affinity, and the R (relaxed) state, which has a high oxygen affinity. The T↔R allosteric transition involves a rotation and a shift of one $\alpha1\beta1$ dimer relative to the other symmetry-related $\alpha2\beta2$ dimer. This movement results in the disruption and/or formation of a new hydrogen bond and salt-bridge interactions across the $\alpha1\beta2$ (and symmetry-related $\alpha2\beta1$) dimer interfaces. The T-state has significantly more hydrogen-bond/salt interactions bridging the $\alpha1\beta2$ interface than are found in the R-state structure. Disruption of any of the $\alpha1\beta2$ interface bonds that stabilize the T state causes high oxygen affinity (Rosemeyer & Huehns, 1967; Perutz *et al.*, 1968) and *vice versa*. Thus, most mutations in the $\alpha1\beta2$ interface either cause an increase or a decrease in oxygen affinity, leading to polycythemia or anemia, methemoglobinemia, cyanosis, tissue hypoxia and respiratory distress (Dincol *et al.*, 1994; Schroeder

et al., 1979; Borg *et al.*, 1997; Kister *et al.*, 1995; Schneider *et al.*, 1975; Bonaventura & Riggs, 1968; Reissmann *et al.*, 1961; Efremov *et al.*, 1978; Winslow & Charache, 1975; Arous *et al.*, 1981).

Hb Bassett is a mutant Hb that was first described by V. N. Fairbanks in a personal communication in Huisman *et al.* (1996); however, detailed studies were not reported. Recently, Abdulmalik *et al.* (2004) published detailed functional studies of their analysis of Hb Bassett identified in a six-year-old Caucasian patient. The properties of this variant included a very low oxygen affinity in stripped Hb solutions at pH 7.0 [P_{50} of 22.0 mmHg (2933 Pa) in Hb Basset, compared with 10.5 mmHg (1400 Pa) in HbA], episodic cyanosis and reduced hemoglobin stability. Mass spectrometry and amino-acid analysis revealed an αAsp94→Ala substitution. This mutation was confirmed by DNA sequencing of the α-globin gene, which revealed a single nucleotide change (G**A**C→G**C**C). Crystallographic studies were initiated to determine mechanistically at the molecular level the functional differences between Hb Bassett and HbA.

2. Materials and methods

2.1. Purification, crystallization, X-ray data collection and processing

Hb Bassett was separated from the patient's total Hb and purified as previously reported (Abdulmalik *et al.*, 2004). For the R-state crystallization experiment, Hb solution was evacuated for about 10 min and the resulting deoxygenated solution was further reduced by the addition of a small pellet of $Na_2S_2O_4$. The fully reduced deoxygenated Hb (deoxyHb) solution was then saturated with CO to generate the CO-bound Hb form. Crystallization was carried out with a solution of 40 mg ml^{-1} protein and 3.4 *M* phosphate buffer (0.45 volumes of 4 *M* K_2HPO_4, 0.55 volumes of 4 *M* NaH_2PO_4 and 0.18 volumes of water, pH 6.7) using 2 ml test tubes as previously described (Perutz, 1968; Safo & Abraham, 2003). A drop of toluene was added to the Hb solution in each tube. Additional CO was bubbled into the tubes and they were sealed. R-state crystals appeared in several of the tubes containing 2.25–2.75 *M* phosphate after 4–10 d.

For the T-state crystallization experiment, Hb solution was evacuated for about 30 min and the resulting deoxyHb solution was further reduced by the addition of a small pellet of $Na_2S_2O_4$. Subsequent crystallization of the Hb solution in 2 ml test tubes using 3.2–3.6 *M* sulfate/phosphate buffer [0.8 volumes of 4 *M* $(NH_4)_2SO_4$, 0.05 volumes of 2 *M* $(NH_4)H_2PO_4$ and 0.15 volumes of 2 *M* $(NH_4)_2HPO_4$ pH 6.5] was performed in a glove box under a nitrogen atmosphere as previously described (Perutz, 1968; Safo & Abraham, 2003). T-state crystals appeared after 2–5 d.

Diffraction data sets for both the R- and T-state crystals of Hb Bassett were collected at 100 K using a Molecular Structure Corporation (MSC) X-Stream Cryogenic Crystal Cooler System (MSC, The Woodlands, TX, USA), an R-AXIS II image-plate detector equipped with Osmic confocal mirrors and a Rigaku RU-200 X-ray generator operating at 50 kV and 100 mA. The space groups for the R- and T-state mutant crystals are $P4_12_12$ and $P2_1$ and are isomorphous to those of high-salt R- and T-state Hb crystals, respectively. Prior to their use in X-ray diffraction, the crystals were first washed in a cryoprotectant solution containing 50–60 µl mother liquor and 8–15 µl glycerol. The data sets were processed with the MSC *BIOTEX* software program. Data-collection and processing statistics for both crystals are summarized in Table 1.

2.2. Structure determination and refinement

The isomorphous $\alpha1\beta1$ R-state (PDB code 1aj9) and $\alpha1\beta1$-$\alpha2\beta2$ T-state (PDB code 2hhb) HbA structures without water and ligands with *B* factors set to 30 Å were used as starting models to refine the R- and T-state Hb Bassett structures, respectively. The normal αAsp94 residue was mutated to Gly.

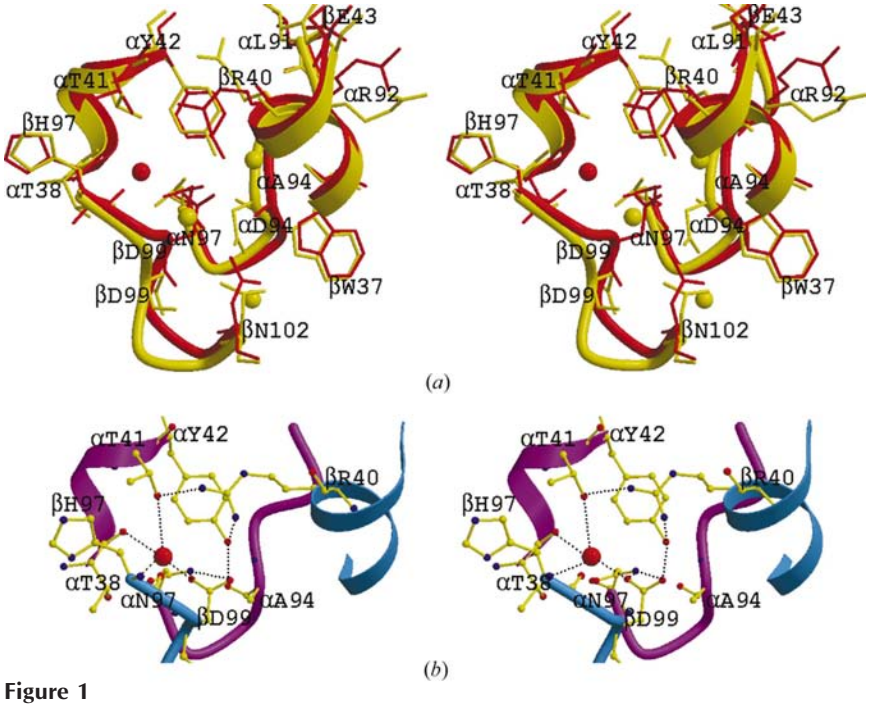

Figure 1
Stereo figure of the $\alpha1\beta2$ dimer interface of R-state Hb. The residues are shown in ribbons and/or ball-and-stick representation. Water molecules are shown as spheres, while hydrogen bonds are represented by dashed lines. (*a*) Superposition of the $\alpha1\beta2$ dimer interface of Hb Bassett (red) and HbA (yellow). The structures were superimposed using the invariant $\alpha1\beta1$ dimer (C^α residues) on the BGH frame (see text). (*b*) The $\alpha1\beta2$ dimer interface of Hb Bassett showing intersubunit hydrogen-bonding interactions (see Table 2 for values). The $\alpha1$-subunit and $\beta2$-subunit are in magenta and cyan, respectively. O and N atoms are in red and blue, respectively. Some side chains are omitted for clarity. The figures were generated with *MOLSCRIPT* (Kraulis, 1991) and *RASTER3D* (Merritt & Murphy, 1994) and labeled with *SHOWCASE*.

Table 1
Data-collection and refinement statistics for Hb Bassett.

Values in parentheses refer to the outermost resolution bin.

	R (Bassett)	T (Bassett)
Data collection		
Space group	$P4_12_12$	$P2_1$
Unit-cell parameters (Å, °)	a = 53.36, b = 53.36, c = 191.78	a = 62.47, b = 82.23, c = 53.56, β = 100.2
Resolution limits (Å)	2.15 (2.20–2.15)	1.80 (1.85–1.80)
No. of reflections	14996 (739)	47432 (3072)
Redundancy	5.8 (2.8)	2.9 (2.0)
$I/\sigma(I)$	15.0 (2.1)	13.1 (1.6)
Completeness (%)	93.8 (72.4)	93.9 (77.5)
$R_{\rm merge}$† (%)	7.5 (31.2)	7.3 (36.6)
Structure refinement		
Resolution limit (Å)	51.41–2.15 (2.28–2.15)	49.24–1.80 (1.91–1.80)
No. of reflections (no σ cutoff)	14996 (1991)	47413 (6708)
R factor (%)	22.2 (26.5)	18.3 (33.2)
$R_{\rm free}$‡ (%)	28.8 (30.3)	23.6 (37.3)
R.m.s.d. from standard geometry		
Bond lengths (Å)	0.009	0.013
Bond angles (°)	1.9	1.7
Average B values (Å^2)		
Protein/heme atoms	40.9/38.9	32.0/28.9
Water	47.1	43.9
Others	49.2 (toluene)	74.5 (sulfate)
Ramachandran plot (%)		
Most favored/additional	90.0/10.0	93.4/6.6

† $R_{\rm merge} = \sum\langle I\rangle - I/\sum I$. ‡ 5% of the reflections, which were used for the calculation of $R_{\rm free}$, were excluded from the refinement.

The refinements were performed with the *CNS* program (Brünger *et al.*, 1998), with bulk-solvent correction applied.

The starting R-state model was subjected to rigid-body refinement with the two Hb subunits treated as independent groups using all crystallographic data to 2.15 Å. The model was then subjected to alternate runs of positional, simulated-annealing and individual B-factor refinement and addition of water, with intermittent manual model corrections. In particular, manual adjustments at the $\alpha1\beta2$ dimer interface where the mutation occurs were made as it differs significantly from the native region. Alanine at position α94 became apparent in the density map and the side chain was built into the model. The two hemes were also fitted with CO ligands. The final model contained 192 water molecules and two toluene molecules with a final R factor and $R_{\rm free}$ of 22.2 and 28.8%, respectively.

The starting T-state model was subjected to a round of rigid-body conjugate-gradient minimization, simulated-annealing and individual B-factor refinement. Alanine at position α94 became apparent in the density maps and was built into the model. The mutation sites of the T-state Hb Bassett and T-state HbA were very similar and only limited adjustments were made. Several alternate rounds of positional, simulated-annealing and individual B-factor refinement and the addition of two sulfate anions and 596 water molecules, with intermittent manual model corrections, brought the final R factor and $R_{\rm free}$ to 18.3 and 23.6% at 1.80 Å resolution, respectively.

Model building and correction were carried out using the program *TOM* (Cambillau & Horjales, 1987). The model was also subjected to quality analysis during the various refinement stages with omit maps. Refinement statistics are summarized in Table 1.

3. Results

3.1. Crystal structures of R- and T-state Hb Bassett

The R- and T-state Hb Bassett crystal structures were determined at 2.15 and 1.80 Å and are isomorphous with the R- and T-state HbA structures (PDB codes 1aj9 and 2hhb), respectively. Table 1 provides the crystallographic parameters that were observed for both mutant structures. The R-state Hb Bassett asymmetric unit encompasses one $\alpha1\beta1$ dimer and the T-state Hb Bassett a tetramer ($\alpha1\beta1$-$\alpha2\beta2$). The R-state tetramer was generated using crystallographic symmetry operations. The $2F_{\rm o} - F_{\rm c}$ electron-density maps at 1.0σ for both the R- and T-state mutant were well defined for the entire polypeptide main-chain atoms, with the exception of the R-state α N- and C-termini (αVal1 and αArg141), similar to native HbA.

Interestingly, toluene, which was used to aid in the crystallization process, binds to the R-state Hb Bassett at two locations within a hydrophobic pocket formed by αTrp14, αVal17, αAla21, αTyr24, αLeu105, αLeu109, αLeu129, αLeu125, αPhe128, αVal10, αVal70 and αLeu66. The aromatic rings of the two toluene molecules are stacked on top of each other. The toluene-binding site was first identified by Schoenborn (1976) by the binding of the antigelling agent dichloromethane. Later, Abraham *et al.* (1982) also observed binding of the antigelling compounds iodobenzene and *p*-BrBzIOH at this site. The basis for the antigelling activity of these compounds is not yet fully understood. It has been proposed that because αTrp14 lies close to αHis20, which makes a hydrogen bond with βGlu22 of a neighboring molecule along a single fibre of sickle-cell Hb, binding of any compound near αTrp14 may help to destabilize the formation of a polymer (Schoenborn, 1976; Wishner *et al.*, 1975; Benesch *et al.*, 1977).

3.2. Structural differences between R-state Hb Bassett and R-state HbA

The programs *ALIGN* (Cohen, 1997) and *LSQKAB* as implemented in the *CCP*4 program suite (Collaborative Computational Project, Number 4, 1994) were used for structure alignment and comparison. The mutant dimer ($\alpha1\beta1$) and tetramer ($\alpha1\beta1$-$\alpha2\beta2$) conformations superimpose on the R-state HbA structure with r.m.s.d.s of 0.49 and 0.65 Å for 274 and 236 pairs of C^α atoms, respectively. The tetramer structures were superimposed using the invariant C^α residues ($\alpha1\beta1$-$\alpha2\beta2$) on the BGH frame as defined by Baldwin & Chothia (1979). Although the r.m.s.d. values indicate similar tertiary and quaternary structures, there are several notable differences between the two R structures at the mutation site of the $\alpha1\beta2$ dimer interface and also at the β-cleft. Firstly, two key R-state Hb $\alpha1$ to $\beta2$ interactions (α1Asp94 to β2Asn102

and α1Asp94 to β2Trp37) are abolished in R-state Hb Bassett as a result of the substitution of αAsp94 with Ala (Table 2).

Secondly, there is considerable weakening of a diagnostic R-state Hb hydrogen-bond interaction (α1Thr38 OG1 to β2His97 O) as the side chain of α1Thr38 is now disordered in two positions. In one position (refined), the native R-state HbA interaction between β2His97 O and α1Thr38 OG1 is no longer observed in the mutant R structure. Rather, we observe in the mutant structure a single water molecule that links the α-chain residues α1Thr38 and α1Thr41 to the β-chain residues β2His97 and β2Asp99 (Table 2). In the second disordered position of the α1Thr38 side chain (not refined), we observe a very weak direct hydrogen-bonding interaction (~3.7 Å) between α1Thr38 and β2His97 in addition to the above water-mediated interactions. A similar observation, also involving a disordered α1Thr38, was recently reported in a CO-liganded HbA structure, which the authors attributed to an initiation of the allosteric transition from R-state to T-state (Safo *et al.*, 2002).

Thirdly, there is a large conformational change at the β2-FG corner of R-state Hb Bassett, where residues β2Val98–β2Asn102 have rotated and shifted closer to the α1-C helix (residues α1Leu91–α1Asn97) (Fig. 1*a*). It seems that the positions of the α-C helix and β-FG corner are dictated by the two acidic residues α1Asp94 and β2Asp99. These two residues are opposite each other across the dimer interface in native R-state HbA and we hypothesize that repulsion between them forces the α-C helix and β-FG corner to move apart and occupy the positions observed in the native structure, whilst in the mutant structure the repulsion is removed *via* the mutation of αAsp94 to Ala, causing the two subunits to close in on each other. This closure has resulted in the formation of two new hydrogen bonds in the mutant structure (α1Tyr42–β2Asp99 and α1Asn97–β2Asp99; Table 2, Fig. 1*b*). Remarkably, these newly formed hydrogen bonds that are absent in the native R-state HbA structure are present in T-state HbA and are diagnostics of T-state Hb structures (Table 2).

Fourthly, a weak hydrogen-bond interaction (3.6 Å) found between α1Arg92 O and β2Arg40 NE in R-state HbA is missing in the mutant R structure (Table 2). Overall, six direct and three water-mediated hydrogen-bond interactions are found at the $\alpha1\beta2$ interface of R-state HbA, compared with four or five (including the weak hydrogen-bond interaction between the disordered α1Thr38 and β2His97) direct and two water-mediated hydrogen bonds in R-state Hb Bassett (Table 2).

Table 2
Specific bonds at the $\alpha1\beta2$ interface of the different Hb states.

The contact distances shown (in Å) are those between the $\alpha1\beta2$ interface. Similar distances are also observed at the symmetry-related $\alpha2\beta1$ contact region. Only hydrogen-bond distances $\leq$ 3.6 Å are shown.

(*a*) Direct protein interactions.

Contact		R (1aj9)	R (Bassett)	T (2hhb)	T (Bassett)
α1Thr38 OH	β2His97 O	2.4	—	—	—
α1Tyr42 OH	β2Asp99 OD1	—	2.7	2.5	2.7
α1Thr41 OH	β2Arg40 NH2	2.9	2.6	—	—
α1Tyr42 OH	β2Arg40 NH1	2.9	3.3	—	—
α1Asp94 OD2	β2Asn102 ND2	3.2	—	—	—
α1Asp94 OD1	β2Trp37 NE1	3.3	—	3.0	—
α1Leu91 O	β2Arg40 NE	—	—	2.8	3.4
α1Asn97 ND2	β2Asp99 OD1	—	3.0	2.8	2.8
α1Arg92 O	β2Arg40 NE	3.6	—	3.3	—
α1Arg92 NH2	β2Glu43 OE2	—	—	—	3.0
α1Lys40 NZ	β2His146 OXT	—	—	2.5	2.6
α1Arg141 NH1	β2Val34 O	—	—	2.9	2.9

(*b*) Water-mediated interactions.

Contact			R (1aj9)	R (Bassett)	T (2hhb)	T (Bassett)
α1Pro37 O	wat1	β2His146 OXT	—	—	2.9:2.5	2.9:2.8
α1Thr38 OG1	wat2	β2Asp99 OD2	—	—	2.8:2.7	2.7:2.8
α1Thr41 OG1	wat3	β2Arg40 NH1	—	—	2.7:2.9	2.9:3.0
α1Tyr42 OH	wat4	β2Asn102 ND2	—	—	3.1:3.0	2.6:2.9
α1Tyr42 O	wat5	β2Arg40 NH2	—	—	2.7:3.0	2.7:3.1
α1Arg92 NH1	wat6	β2Gln39 OE1	—	—	3.1:3.3	3.6:2.6
α1Asn97 OD1	wat2	β2Asp99 OD2	—	—	2.7:2.7	2.7:2.8
α1Tyr140 O	wat7	β2Trp37 N	—	—	2.9:3.5	2.9:3.4
α1Arg92 O	wat8	β2Trp37 O	—	—	—	2.7:2.6
α1Val96 N	wat9	β2Glu43 OE2	—	—	—	3.1:3.1
α1Asp94 OD2	wat10	β2Glu101 OE2	—	—	2.9:3.6	—
α1Asp94 OD2	wat11	β2Asn102 ND2	2.7:3.4	—	2.8:2.7	—
α1Tyr42 OH	wat12	β2Trp37 O	2.7:3.2	—	—	—
α1Asp94 OD2	wat13	β2Asn99 N	3.4:3.2	—	—	—
α1Thr38 O	wat14	β2His97 O	—	2.7:2.5	—	—
α1Thr41 OG1	wat14	β2Asp99 OD2	—	3.2:2.5	—	—

Finally, another striking difference between R-state Hb Bassett and R-state HbA involves the interactions associated with linking the β-subunits. The well defined C-termini of R-state Hb Bassett show βAsn139 and βHis146 and their symmetry-related counterparts involved in hydrogen-bonding interactions (Fig. 2*a*). In contrast, there are no apparent interactions between βAsn139 and βHis146 in the R-state HbA structure, as the side chains of these two residues have reoriented away from each other (Fig. 2*b*).

3.3. Structural differences between T-state Hb Bassett and T-state HbA structures

Comparison of T-state Hb Bassett and T-states HbA structures shows very similar tertiary and quaternary structures, with r.m.s.d.s of 0.29 and 0.36 Å, respectively, for 270 and 236 pairs of C^{α} atoms. Unlike the mutant R structure, the removal of the repulsive interaction caused by α1Asp94–β2Asp99 at the $\alpha1\beta2$ dimer interface does not seem to lead to any significant structural changes in the T-state mutant (Fig. 3). However, as a result of the replacement of βAsp94 with Ala, the T-state HbA hydrogen-bonding interaction

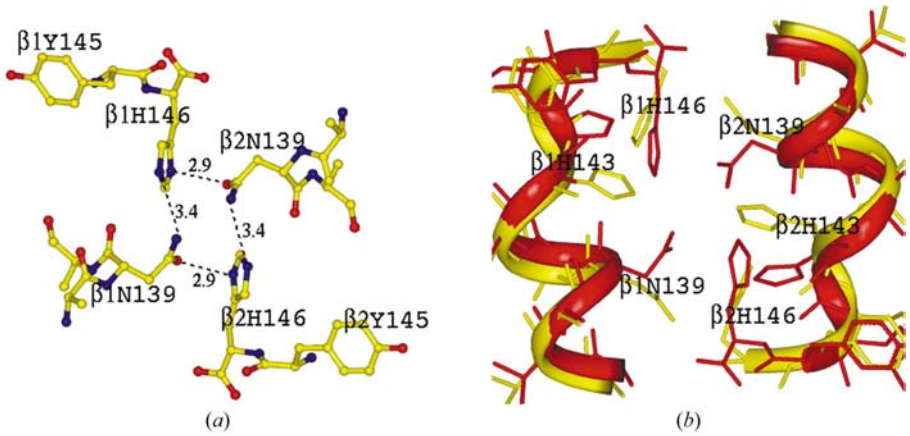

Figure 2
The β-cleft of R-state Hb. The residues are shown in ribbons and/or ball-and-stick representation. Hydrogen bonds are represented by dashed lines. (*a*) Hb Bassett showing αAsn139 and βHis146 and their symmetry-related counterparts intimately involved in hydrogen-bonding interactions. O and N atoms are in red and blue, respectively. (*b*) Superposition of the β-cleft of Hb Bassett (red) and HbA (yellow). The structures were superimposed using the invariant $\alpha1\beta1$ dimer (C^{α} residues) on the BGH frame (see text). The figures were generated with *INSIGHT*II (Molecular Simulations, Inc., San Diego, CA, USA) and labeled with *SHOWCASE*.

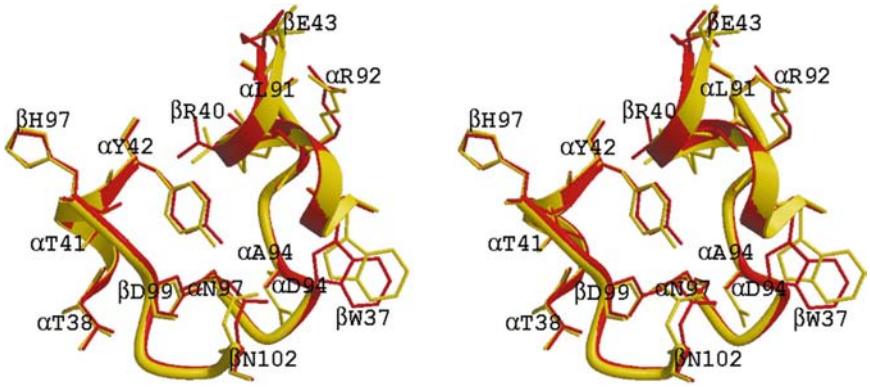

Figure 3
Stereo figure of the superposition of the $\alpha1\beta2$ dimer interface of T-state Hb Bassett (red) and T-state HbA (yellow). The residues are shown in ribbons and/or sticks. Water molecules and some side chains are omitted for clarity. The structures were superimposed using the invariant $\alpha1\beta1$ dimer (C^{α} residues) on the BGH frame (see text). The figures were generated with *MOLSCRIPT* (Kraulis, 1991) and *RASTER3D* (Merritt & Murphy, 1994) and labeled with *SHOWCASE*.

between α1Asp94 and β2Trp37 is absent in the mutant (Table 2). Interestingly, a hydrogen bond in the T-state HbA between the carbonyl O atom of α1Arg92 and the guanidinium group of β2Arg40 is now replaced in Hb Bassett by a salt-bridge interaction between the side chains of α1Arg92 and β2Glu43. We believe that the difference in the Hb Bassett α1Arg92 contact is a normal variant interaction found in other high-resolution native T-state Hb structures (PDB codes 1a3n, 1bz0, 1thb and 1ljw) and is most likely to arise from the flexibility of the side chains of βArg40 and βGlu43 and is not a consequence of the mutation.

There are seven hydrogen-bonding and salt-bridge interactions found at the $\alpha1\beta2$ interface of the T-state HbA structure, compared with six for the T-state Hb Bassett structure. There are a total of ten water-mediated hydrogen-bonding interactions across the $\alpha1\beta2$ interface in both the native and mutant T-state Hb structures; eight of them are conserved, while two are unique to each structure. Thus, the structural change at the $\alpha1\beta2$ dimer interface of T-state Hb Bassett is minimal, with the exception of the loss of one hydrogen bond at the $\alpha1\beta2$ dimer interface.

4. Discussion

4.1. Understanding the functional properties of Hb Bassett

Detailed functional studies (Abdulmalik *et al.*, 2004) with Hb Bassett solutions demonstrate the mutant to have a markedly reduced oxygen affinity compared with that of HbA (P_{50} at pH 7.0 = 22.0 mmHg compared with 10.5 mmHg in HbA), a reduced Bohr effect (−0.26 compared with −0.54 in HbA) and a low subunit cooperativity (n = 1.4 compared with 2.6 in HbA). In addition, Hb Bassett is slightly unstable compared with HbA.

In general, the $\alpha1\beta2$ (and corresponding $\alpha2\beta1$) dimer interfaces of any Hb tetramer are important structural features that control the allosteric transition between the R and T states. It is therefore no surprise that the $\alpha1\beta2$ contact mutant substitution (αAsp94→Ala) causes a significant effect on the functional properties in this variant. For example, Hb Kansas (βAsn102→Thr), Hb Saint Mandé (βAsn102→Tyr), Hb Setif (αAsp94→Tyr), Hb Çapa (αAsp94→Gly) and Hb Titusville (αAsp94→Asn) result in a low-affinity Hb (Bonaventura & Riggs, 1968; Bordahandy & Rosa, 1981; Borg *et al.*, 1997; Webber *et al.*, 1994; Schneider *et al.*, 1975; Huisman *et al.*, 1996), while other mutations at the $\alpha1\beta2$ interface show an increased oxygen affinity, *i.e.* Hb Beth Israel (βAsn102→Ser), Hb Richmond (βAsn102→Lys) and Hb Roanne (αAsp94→Glu) (Efremov *et al.*, 1978; Winslow & Charache, 1975; Kister *et al.*, 1995).

The high-resolution structures presented in this study provide detailed descriptions of both R- and T-state Hb Bassett that can be compared with native HbA structures in order to explain the observed functional properties of Hb Bassett. The allosteric transition from R to T in native Hb creates two new $\alpha1\beta2$ dimer intersubunit interactions (α1Tyr42–β2Asp99 and α1Asn97–β2Asp99; Table 2). Remarkably, these same two T-state HbA diagnostic hydrogen-bonding interactions that are absent in native R structures are observed in R-state Hb Bassett. Moreover, the hydrogen-bonding interaction associated with αAsp94 in the

native R structure (α1Asp94–β2Asn102) is missing in both the R-state mutant and T-state HbA structures. It thus appears that the mutant R structure has assumed T-state features, consistent with the observed low-oxygen affinity of Hb Bassett. Additionally and as previously pointed out by Safo *et al.* (2002), the weakening of the R-state hydrogen-bonding interaction between α1Thr38 and β2His97 in the R-state mutant structure also serves to confer T-state characteristics on the mutant R structure. Significantly, the removal of the interdimer repulsion involving α1Asp94 and β2Asp99 in Hb Bassett should result in lower affinity for oxygen. Abraham *et al.* (1997) have previously shown that negative polar interactions are as important as salt bridges and hydrogen bonds in shifting the allosteric properties in Hb.

The apparent reduction in hydrogen-bonding interactions across the $\alpha1\beta2$ dimer interface in the mutant Hb compared with native HbA may explain the low cooperativity as well as the slight instability of Hb Bassett. On the other hand, one would predict that the weakening of the T-state Hb Bassett $\alpha1\beta2$ dimer interface should cause an increase in oxygen affinity. Undoubtedly, this effect is offset by the T-state characteristics of the R-state Hb Bassett, as well as the removal of the negative polar interaction (caused by α1Asp94–β2Asp99) across the dimer interface in the mutant Hb.

The Bohr effect (oxygenation-linked changes in proton binding) plays a significant role in the allosteric regulation of Hb (Perutz, 1970). Kilmartin *et al.* (1978) found that 40% of the Bohr effect arises from salt-bridge interactions between βHis146 and βAsp94 in T-state Hb, which leads to the uptake of a proton by βHis146. The allosteric shift to R-state Hb opens this salt bridge and βHis146 becomes highly solvated (Perutz, 1970). As a result the imidazole pK_a is reduced from 8.0 in deoxygenated Hb to 7.1 in liganded Hb (Kilmartin *et al.*, 1973), with a concomitant release of a proton and an increase in oxygen affinity. Interestingly, in the R-state Hb Bassett structure, βHis146 is ordered and both N^{δ} and N^{ϵ} of the βHis146 imidazole are involved in hydrogen-bonding interactions with the two symmetry-related βAsn139 residues, characteristic of the T-state diagnostic interaction between βHis146 and βAsp94. It is plausible to assume that these interactions are accompanied by protonation of the βHis146 imidazole N atoms and should lower the Bohr effect and further decrease the affinity of Hb Bassett for oxygen, consistent with the observed properties of the mutant. Also, linking the β-subunits, similar to the action of the natural allosteric effector 2,3-diphosphoglyceric acid (2,3-DPG), should produce a low-affinity Hb. Interestingly, a recently published R-state HbA structure was found to have T-state characteristics, which the authors partially attributed to an interaction between a phosphate molecule and βHis146 at the β-cleft similar to the effects of the binding of 2,3-DPG in T-state Hb (Safo *et al.*, 2002).

In summary, the substitution of βAsp94 with Ala leads to formation of three unique hydrogen-bonding interactions in the R-state mutant: two of them at the $\alpha1\beta2$ dimer interface (α1Tyr42–β2Asp99 and α1Asn97–β2Asp99) and one at the β-cleft (β1His146–β2Asn139). These interactions serve to confer T-state characteristics on R-state Hb Bassett. In addition to these newly created hydrogen bonds in the R-state, the mutation also leads to reduction in the number of intersubunit hydrogen-bonding contacts in both R- and T-state Hb Bassett as well as the removal of the repulsive interactions caused by αAsp94–βAsp99 found in HbA. The combination of these structural features appears to account for the observed functional properties of Hb Bassett.

We gratefully acknowledge research support from NIH to MKS (grant HL04367).

References

Abdulmalik, O., Safo, M. K., Lerner, N. B., Ochotorena, J., Daikhin, E., Abraham, D. J. & Asakura, T. (2004). *Am. J. Hematol.* **77**, 268–276.

Abraham, D. J., Kellogg, G. E., Holt, J. M. & Ackers, G. K. (1997). *J. Mol. Biol.* **272**, 613–632.

Abraham, D. J., Mehanna, A. S. & Williams, F. L. (1982). *J. Med Chem.* **25**, 1015–1017.

Arous, N., Braconnier, F., Thillet, J., Blouquit, Y., Galacteros, F., Chevrier, M., Bordahandy, C. & Rosa, J. (1981). *FEBS Lett.* **126**, 114–116.

Baldwin, J. & Chothia, C. (1979). *J. Mol. Biol.* **129**, 175–220.

Benesch, R. E., Kwong, S., Benesch, R. & Edjali, R. (1977). *Nature (London)*, **269**, 772–775.

Bonaventura, J. & Riggs, A. (1968). *J. Biol. Chem.* **243**, 980–991.

Bordahandy, C. & Rosa, J. (1981). *FEBS Lett.* **126**, 114–116.

Borg, I., Valentino, M., Fiorini, A. & Felice, A. E. (1997). *Hemoglobin*, **21**, 91–96.

Brünger, A. T., Adams, P. D., Clore, G. M., DeLano, W. L., Gros, P., Grosse-Kunstleve, R. W., Jiang, J.-S., Kuszewski, J., Nilges, M., Pannu, N. S., Read, R. J., Rice, L. M., Simonson, T. & Warren, G. L. (1998). *Acta Cryst.* D**54**, 905–921.

Cambillau, C. & Horjales, E. (1987). *J. Mol. Graph.* **5**, 174–177.

Cohen, G. E. (1997). *J. Appl. Cryst.* **30**, 1160–1161.

Collaborative Computational Project, Number 4 (1994). *Acta Cryst.* D**50**, 760–763.

Dincol, G., Dincol, K., Erdem, S., Pobedimskaya, D. D., Molchanova, T. P., Ye, Z., Webber, B. B., Wilson, J. B. & Huisman, T. H. (1994). *Hemoglobin*, **18**, 57–60.

Efremov, G. D., Stojmirovic, E., Lam, H. L., Wilson, J. B. & Huisman, T. H. (1978). *Hemoglobin*, **2**, 75–77.

Huisman, T. H., Carver, M. F. & Efremov, G. D. (1996). *A Syllabus of Human Hemoglobin Variants.* Augusta, GA, USA: The Sickle Cell Anemia Foundation.

Kilmartin, J. V., Breen, J. J., Roberts, G. C. & Ho, C. (1973). *Proc. Natl Acad. Sci. USA*, **4**, 1246–1249.

Kilmartin, J. V., Imai, K., Jones, R. T., Faruqui, A. R., Fogg, J. & Baldwin, J. M. (1978). *Biochim. Biophys. Acta*, **534**, 15–25.

Kister, J., Kiger, L., Francina, A., Hanny, P., Szymanowicz, A., Blouquit, Y., Prome, D., Galacteros, F., Delaunay, J. & Wajcman, H. (1995). *Biochim. Biophys. Acta*, **1246**, 34–38.

Kraulis, P. J. (1991). *J. Appl. Cryst.* **24**, 946–950.

Merritt, E. A. & Murphy, M. E. P. (1994). *Acta Cryst.* D**50**, 869–873.

Perutz, M. F. (1968). *J. Cryst. Growth*, **2**, 54–56.

Perutz, M. F. (1970). *Nature (London)*, **228**, 726–734.

Perutz, M. F., Muirhead, H., Cox, J. M. & Goaman, L. C. (1968). *Nature (London)*, **219**, 131–139.

Rosemeyer, M. A. & Huehns, E. R. (1967). *J. Mol. Biol.* **25**, 253–273.

Reissmann, K. R., Ruth, W. E. & Nomura, T. (1961). *J. Clin. Invest.* **40**, 1826–1833.

Safo, M. K. & Abraham, D. J. (2003). *Hemoglobin Disorders, Molecular Methods and Protocols*, Vol. 82, edited by R. L. Nagel, pp. 1–19. Totowa, NJ, USA: Humana Press Inc.

Safo, M. K., Burnett, J. C., Musayev, F. N., Nokuri, S. & Abraham, D. J. (2002). *Acta Cryst.* D**58**, 2031–2037.
Schneider, R. G., Atkins, R. J., Hosty, T. S., Tomlin, G., Casey, R., Lehmann, H., Lorkin, P. A. & Nagai, K. (1975). *Biochim. Biophys. Acta*, **400**, 365–373.
Schoenborn, B. P. (1976). *Proc. Natl Acad. Sci. USA*, **73**, 4195–4199.
Schroeder, W. A., Shelton, J. B., Shelton, J. R. & Powars, D. (1979). *Hemoglobin*, **3**, 145–159.
Webber, B. B., Wilson, J. B. & Huisman, T. H. (1994). *Hemoglobin*, **18**, 57–60.
Winslow, R. M. & Charache, S. (1975). *J. Biol. Chem.* **250**, 6939–6942.
Wishner, B. C., Ward, K. B., Lattman, E. E. & Love, W. E. (1975). *J. Mol. Biol.* **98**, 179–194.